



# An innovative signal processing technique for the extraction of ants' walking signals

Sebastian OBERST<sup>1</sup>; Enrique NAVA-BARO<sup>1,2</sup>; Joseph C.S. LAI<sup>1</sup>; Theodore A. EVANS<sup>3</sup>

<sup>1</sup> Acoustics & Vibration Unit, School of Engineering and IT,  
University of New South Wales, ADFA, Canberra, ACT 2600, Australia

<sup>2</sup> Departamento de Ingeniería de Comunicaciones, ETSI Telecomunicación,  
Campus de Teatinos s/n, Universidad de Málaga, 29071 Málaga, Spain

<sup>3</sup> Department of Biological Sciences, National University of Singapore, Singapore 117543

## ABSTRACT

Eusocial insects such as bees, ants and termites communicate multi-modally using chemical, visual, tactile and vibrational cues. While much work has been done on chemical and visual communications, the tactile and vibrational communication channel is somewhat neglected. Recent research indicates that structural vibrations caused by ants can be used to identify their activity level. However, these structural vibrations are caused by the response of the substrate excited by ants walking. The objective of this study is to determine the footprint of ants walking by separating the response of the substrate from the walking signal. The vibration of the substrate (in this case, a wooden veneer) caused by ants walking is measured by a laser vibrometer in an experimental setup isolated from environmental vibrations. By filtering the recorded vibration signal using a technique based on the dynamics in phase space followed by deconvolution from the response of the veneer using TIKHONOV regularisation, the ant's walking signal is extracted and its nature determined.

Keywords: Ant walking signals, vibration, laser vibrometer, deconvolution  
22.6.2 Natural sources of noise (Insects),  
74.9 Signal processing (Other)

## 1. INTRODUCTION

Communication involves the sharing of information (message) via channel (medium e.g. air, water, solid matter) in a meaningful way between sender(s) and recipient(s) (1) and has to be distinguished from simply reading or intercepting signals. Ants (and wasps), termites and bees as eusocial insects rely significantly on efficient means of communication based on pre-filtered information retrieval. While insect communications are naturally multi-modal (2), there are few studies on combined communication channels and researchers concentrate on only the dominant means of information gathering. For ants it is widely acknowledged that chemical means using pheromones is the predominant source of communication (3, 4). Visual communication is also important especially for some more primitive species (5, 6, 7). While it is accepted that termites communicate using substrate vibrations (8, 9), it is debatable for ants in general (10, 11) and only acknowledged in some instances e.g. leaf cutter ants (*Acromyrmex* and *Atta* (12, 13)).

For eusocial insects, other aspects of information gathering become of interest such as interspecies communication or the capability of intercepting signals. Vibration signals perceived as substrate response may be intercepted by e.g. a parasitic species (14, 15). Recently the activity of ants of the species *Iridomyrmex purpureus* has been quantified by vibrations with ants responding to neighbouring nestmates with higher activity levels (16). A classification of vibration excitations according to their response in a wavelet filtered, blind deconvolution inverse process using an accelerometer setup in an anechoic chamber has been limited to only detecting three activities: the falling and impacting of an ant on the substrate, scratching/biting and carrying stones as a combination of the previous two signals (16, 17). The walking response was buried in

<sup>1</sup>s.oberst@adfa.edu.au

<sup>2</sup>en@uma.es

<sup>3</sup>j.lai@adfa.edu.au

<sup>4</sup>theo.evans@nus.edu.sg

noise and the veneer disc was modelled as a generalised linear parametric model in order to deconvolve the excitation signal. Wood is, however, a highly variable anisotropic material (18) and the parametric model might not apply if material nonlinearities are present.

The walking of insects especially cockroaches (19) or stick insects (20) as model organisms has been extensively studied; and has led to the enhanced design of hexapods (21). For ants the most prevalent but possibly one of the most difficult to analyse signals (small amplitude, variability) is that of walking. Excellent experimental studies of the ants stepping pattern and the influence of kinematics, body morphology or load have been published by Zoellikofer (22, 23, 24) comprising twelve species of ants of four genera Formicinae: *Cataglyphis*, *Formica*, *Lasius* and Myrmicinae: *Myrmica*. Results are however based mainly on observations (videos, footprints on smoked glass, geometry) and no vibration detection or excitation signal analysis has been conducted.

Therefore, the present study aims at quantifying the excitation signal extracted from the ants' walking signal vibration response. For this purpose a more sensitive and better environmental vibrations isolated experiment than that used by Oberst et al. (16) has been designed using an air cushion damped laser vibrometer setup in an anechoic chamber. In order to overcome the problem of inversely blind deconvoluting the recorded response, the system's transfer function has been measured first. Then, the ants' walking signal is measured and filtered by making use of the wavelet transform or the dynamics' phase space. The excitation signal is obtained via deconvolution of the response signal with the transfer function of the veneer disc via TIKHONOV regularisation. Results of a median excitation signal of the ant species *Iridomyrmex purpureus* and *Lasius niger* are illustrated.

The process of signal extraction as applied in this study can be summarised as follows:

- 1 Measuring the transfer function of the veneer disc via averaging and its preconditioning
- 2 Filtering the ants' walking response; and
- 3 Excitation signal extraction using *Tikhonov* regularisation (adjustment of regularisation parameter to remedy ill-conditioned matrix division); then reapplication of filter on excitation signal (2).

## 2. EXPERIMENTAL SETUP

The experiments were conducted in an anechoic chamber (150 Hz cut-off frequency, dimensions of  $3 \times 3 \times 3 \text{ m}^3$ ) with controlled temperature of about  $30^\circ\text{C}$  using a temperature calibrated *Sunair* oil fin heater. The humidity could be left uncontrolled as it turned out to be rather constant at a low level of  $28\% \pm 5\%$  RH. The low relative humidity guaranteed that the moisture absorption (25) hence the damping of the wood was kept as low as possible. Temperature measurements, humidity measurements and video recordings were triggered using an ARDUINO UNO setup with temperature and humidity sensor (FREETRONIC, DHT22) and a switch connected to a LED which indicated the recording status.

The setup (lid only of the insect box used in Oberst et al. (16), foam, wood on two bricks) as depicted schematically in Figure 2 was placed in the middle of the anechoic chamber onto foam on a steel frame. However, using a laser vibrometer residual environmental vibrations transmitted through the flooring and omega springs (8 Hz resonance frequency) of the anechoic chamber could be measured and have been identified to originate from personnel walking past the chamber or from impacts of closing steel doors located in neighbouring workshops. Therefore, the steel frame with the lid-setup was isolated from the remaining environmental vibrations using an air-cushioned passive vibration bench top (KINETIC SYSTEMS, Boston, MA ELpF, 24 kg), calibrated at 20 Pa on top of a vibration mat sitting on concrete slabs of 80 kg mass. The pressure of 20 Pa was determined by measuring the impulse response (PSD and amplitude) of a 5 kg weight impact dropped from 0.5 m height on the concrete floor outside the anechoic chamber (distance approximately 1.5m to wall). The location with the highest response sensitivity was taken to vary the pressure of the air-cushioned vibration benchtop in order to minimise effects of footsteps or closing workshop doors (the power per frequency transmitted being of at most of the same order of magnitude as the measured noise floor).

The lid of the insect box was designed of a rectangular PPE container's lid glued to a cylindrical container of radius 25 mm. A veneer disc was placed inside the cylindrical container and then pushed down by a PVC tube (see Oberst et al. (16, 17) for more details on the setup). The measured veneer disc had the following material properties (taken from **Set B** (25)): area of  $2845 \text{ mm}^2$ , weight of 1.3564 g, moisture absorption if exposed to 80% RH of 12.87% relative to dry weight, mode skewness of  $-0.390 \propto 1x$  (measured over light intensity of digital pictures taken).

We applied two thin layers of FLUON (Polytetrafluoroethylene based) to the walls of the PVC tube in order to avoid insects climbing the PVC tube and dropping thus creating 'unnatural behaviour' (c.f. Oberst et al. (16)). The measurements were performed using a single point laser vibrometer POLYTEC PVD-100 with a data

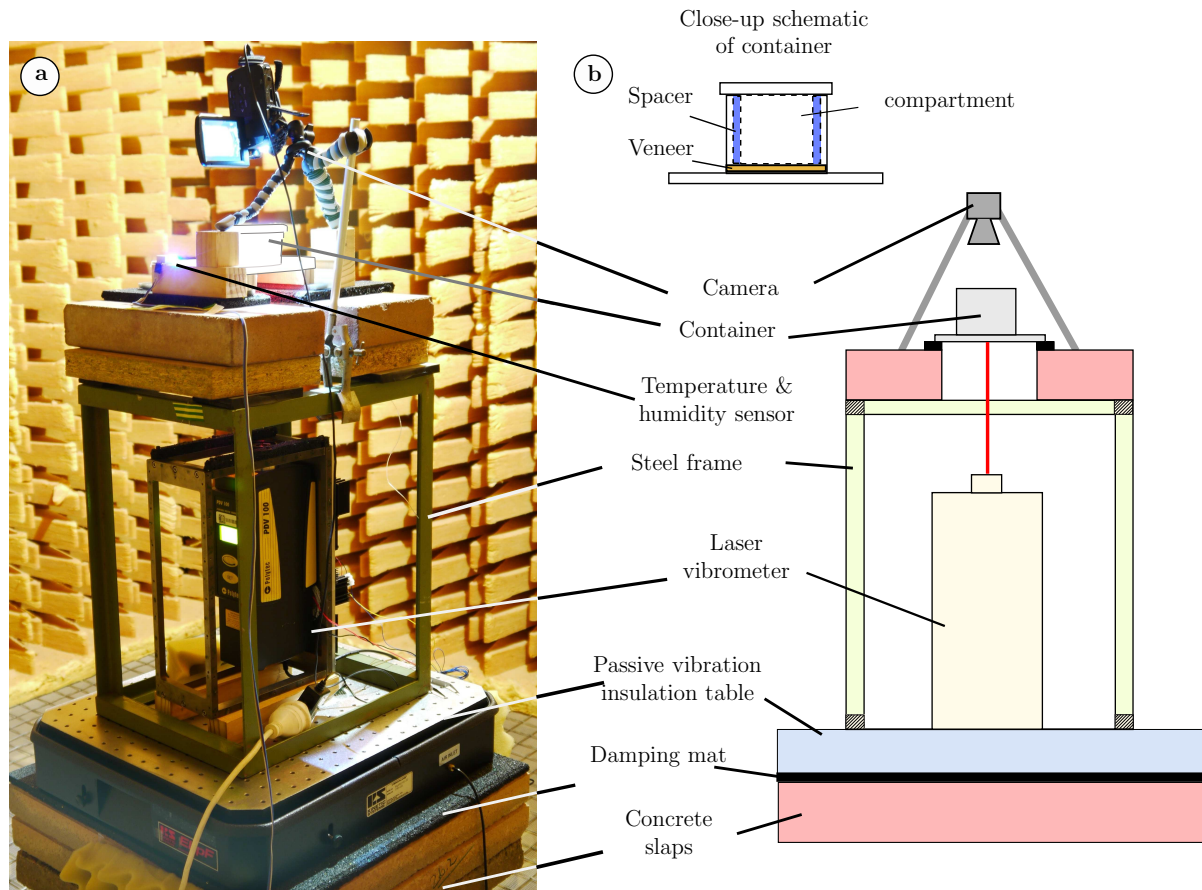


Figure 1 – (a) Experimental setup in anechoic chamber and (b) schematic with closeup of cylindrical container. A passive vibration insulation table and a vibration damping mat were used to eliminate residual environmental vibrations transmitted into the anechoic chamber; vibration is recorded using a laser vibrometer and motion is recorded using a digital video camera

acquisition system Polytec VIB-E-220, connected to a TOSHIBA notebook with Vibsoft 8.8 analysis software. Both the veneer disc and the veneer disc in the lid assembly was measured using  $2^{21}$  samples with a 12 kHz sampling rate. The insects were observed for 172.8 s at the same sampling rate (only  $2^{21}$  for samples). The motion of the specimen in the container (Figure 1) was recorded using a digital video camera BENQ M23 (Full HD 1080p, 30 frames per second) in order to later correlate qualitatively and quantitatively the average activity level and the behaviour to detected vibrations for a larger study. The inside of the container was illuminated during recording using the camera's in-built cool white LED (3 mm). Reference measurements without insects were taken before each measurement in order to determine the noise floor (average RMS value of about  $\sigma = 104 \mu\text{m/s}$ ).

## 2.1 Estimation of transfer function

Firstly, the veneer disc's transfer function (TF) is estimated and, in a second run, the TF of the veneer disc built into the lid assembly is measured in order to conduct at a later stage a de-convolution with the response signal. The setup was excited via loudspeaker (RADIO SHAK, REALISTIC MINIMUS 7) in a  $45^\circ$  angle to the veneer surface in 150 mm minimum distance using a 3 – 6000 kHz rectangular sweep signal at 5 V of 0.5 s length, delayed by 0.01 s (TEKTRONIX AFG 3022 dual channel arbitrary function generator). Using a sampling frequency of 12 kHz,  $2^{23}$  samples were windowed with a  $2^{13}$  samples length textscHann window. A BUTTERWORTH band-pass filter (3 Hz to 4 kHz) with three assumed poles was applied in order to eliminate lower order modes and to concentrate only on the frequency range supported by the loudspeaker's woofer (nominal 100 - 3000Hz).

## 2.2 Measurement of ant vibrations

In a larger study of analysing insect vibrations due to walking 0, 1, 2, 4, 8, 16, 24, 48 and 64 individuals were placed onto the veneer disc and after a cooling off period of about 15 minutes (16), their vibrations

were recorded (each at 12 kHz sampling rate,  $2^{21}$  samples). Here, only vibrations of one individual of two species (*Iridomyrmex purpureus*, *Lasius niger*) are reported. *I. purpureus* is the dominant diurnal ant in Australia and it was chosen due to its widespread distribution and ease of handling (avg. length 8 mm and avg. weight 11.14 mg). *Lasius niger*, also known as the black garden ant found outside Australia, has been studied extensively in the past (22, 26) and is selected here due to its small size (avg. 3 mm) and weight (avg. 1.003 mg), in comparison with *I. purpureus*. Ants were collected from 4 colonies taken from Mt Pleasant (at ADFA, Canberra) and from Binya State Forest, Griffith, NSW, Australia. Reference measurements with zero individuals in the cylindrical container gave an average background noise RMS value of about  $\sigma = 104 \mu\text{m/s}$ . A lower and a higher cut-off frequency of 150 Hz (modes of the anechoic chamber at about 150 Hz) and 5 kHz were used. The average SNR for the walking signal over the three species was 56 dB (measured in highest impact to RMS level of reference measurement) which is well above the SNR below 1 dB (noise equal or higher to signal) for recordings of a similar setup using accelerometers (16).

### 3. EXTRACTION OF ANTS' EXCITATION SIGNALS

#### 3.1 Extraction of the veneer disc's transfer function

The single-sided amplitude spectrum  $\frac{|G(k)|^2}{N}$  (transfer mobility) together with the coherence is depicted in Figure 2.

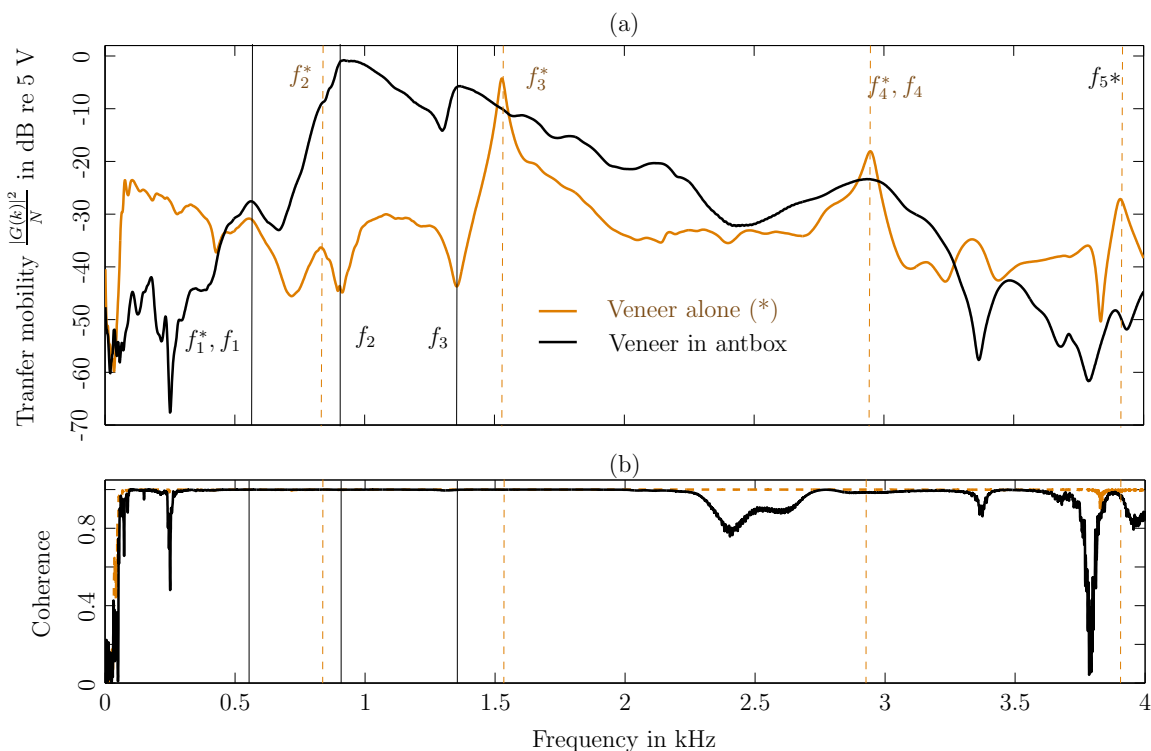


Figure 2 – (a) Transfer mobility of the veneer disc of the veneer disc measured in the centre of the disc. Two resonances  $f_2 = 955.1$  Hz and  $f_3 = 1380$  Hz are dominant. The coherence in (b) indicates that measurements between 0.1 and 3.5 kHz are reliable.

The transfer function of the veneer disc alone gives five resonances at about  $f_1^* = 0.561$ ,  $f_2^* = 0.835$ ,  $f_3^* = 1.527$  (dominant and with 2.81 damping, 3 dB criterion), 2.915 (with 3.0 % damping) and 3.887 kHz (with 2.05 % damping), whereas the transfer function of the veneer disc built into the lid assembly shows about four clear resonances mostly with lower frequencies at about  $f_1 = 0.6$  kHz,  $f_2 = 0.91$  kHz,  $f_3 = 1.4$  kHz and about  $f_4 = 2.93$  kHz (Figure 2). The coherence is mostly unity over the bandwidth of interest, between 0.1 kHz and 3.5 kHz.

#### 3.2 Nonlinear filtering of recorded ant signals

In order to reduce the noise contained in the velocity data measured with the laser vibrometer, recorded signal has been filtered using nonlinear filtering techniques based on phase space reconstruction which is

compared to a wavelet filtered signal (16, 17). The noise is assumed to be additive and independent of the biological signal.

The response signal due to ants walking is embedded using phase space reconstruction techniques (27) and the average auto-mutual information is computed to estimate the signal delay required to get approximately independent embedding vectors. This delay was then used to estimate a suitable global embedding dimension via KENNEL'S false nearest neighbour algorithm (27), in which the dynamics would be able to unfold completely without crossing each other and, therefore, invariants could be calculated and nonlinear filtering techniques based on the dynamics in phase space could be applied. For *I. purpureus* an average delay of  $d = 2.85/12000s = 0.2375$  ms, an embedding dimension of  $m = 8$  has been found and for *L. niger* the delay was  $d = 0.3167$  ms with  $m = 8$ . After having obtained these parameters, the data was nonlinearly filtered using an adaption of the *nrlazy* algorithm (28), source code taken from the TISEAN package (29). The embedded time series was segmented and, for each value  $x_i$ , a set of elements of the trajectory was found for which

$$\mathcal{U}_i^\varepsilon = \{j \mid \|\mathbf{x}_j - \mathbf{x}_i\|_{\text{sup}} < \varepsilon\} \quad (1)$$

The  $\varepsilon$ -threshold has to be chosen large enough to cover the noisy data but still smaller than the average dynamics curvature. Here, a sensitivity study determined that  $\varepsilon = 0.6924\sigma$  ( $\sigma$  standard deviation of the response signal) was large enough to extract the signal. Then, each (central) component was corrected by the average of the values included in the supremum<sup>1</sup>.

$$\hat{x}_i = \frac{1}{|\mathcal{U}_i^\varepsilon|} \sum_{j \in \mathcal{U}_i^\varepsilon} x_j. \quad (2)$$

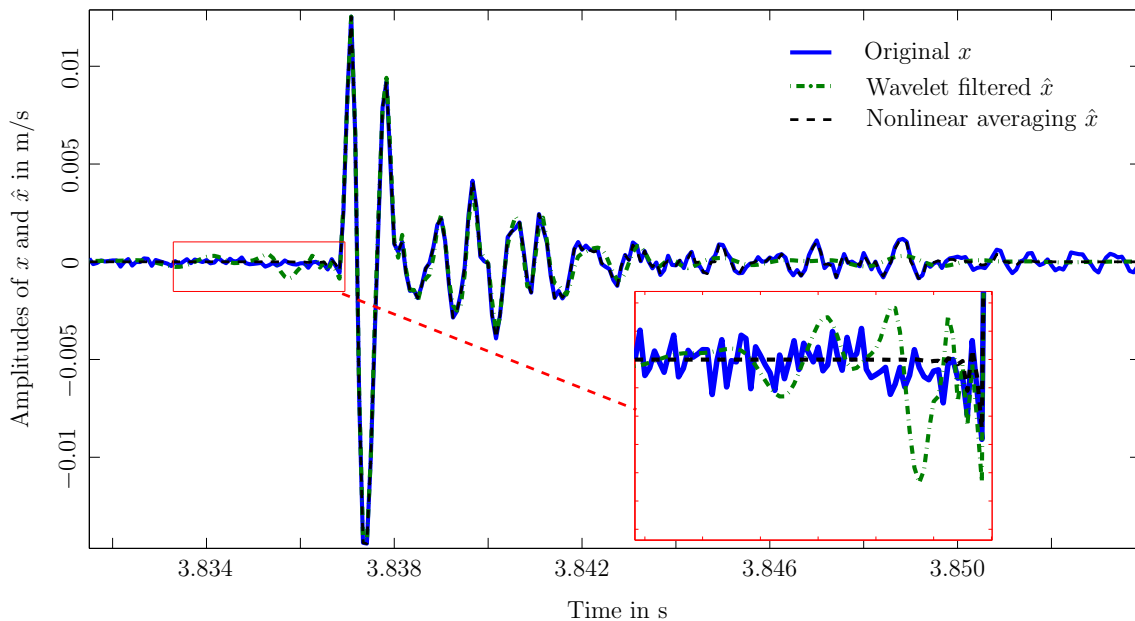


Figure 3 – Original, wavelet filtered (MEYER wavelet) and nonlinearly averaged filtered signal of a small impact. The magnifications show the shortcomings of the different methods: the wavelet based method is influenced by the mother wavelet and the number of scales used.

Also the second statistical moment (variance) was corrected. As the complete time signal was very long and the whole length was required to be analysed later in associated studies, it was segmented into pieces of 50000 samples with the condition that the values of the end points and the subsequent 5 samples were not larger than  $2\sigma$  (the estimated RMS noise level in order to not remove any true impacts), otherwise the time series length was adjusted within a small neighbourhood around the end points. Finally the filtered segments were connected again, reducing computational load of non-linear filtering from 5 days to about 3.5 hours.

As a second filtering method, wavelet filtering based on discrete wavelet transform (16) was applied. First, with a continuous wavelet transform the number of scales to be recorded in synthesising the signal after

<sup>1</sup>Theoretically the supremum is obtained from the subset of neighbours which is the smallest upper bound of neighbours to be included to obtain one recurrent state, e.g. for one 'cycle'.

decomposition had to be determined, based on those scales including at least 90% of the total energy. Here, the discretisation was chosen to go up to level 6 with a synthesised signal making use of up to level 4 scales ( $2^4 = 16$ ). In the discrete wavelet transform, an approximation signal using the MEYER wavelet was computed with an  $\alpha = 1.5$  following the BIRGÉ-MASSART strategy of wavelet coefficient selection.

The filtered result of a small impact time series of walking signal of *I. purpureus* is depicted in Figure 3 (a), together with (b) a comparison of a wavelet filtered signal. Both filtering methods are able to reduce the noise to near-zero amplitude. While the wavelet filtered signal starts to oscillate before the actual excitation (residual mother wavelet), the nonlinearly filtered signal follows more closely the original response. Also, the wavelet based filtering output signal attenuates quicker because of its finite number of (low order) scales. The nonlinear filtering technique takes much more time (3.5 hours compared to a few minutes only for the wavelet based method). The wavelet based approach is less variable for different signals but is also less reliable for responses with small as the noise level amplitudes which can be recovered by the nonlinear filtering approach. It works better for slowly growing and then attenuating responses.

### 3.3 Deconvolution of ants' walking signal

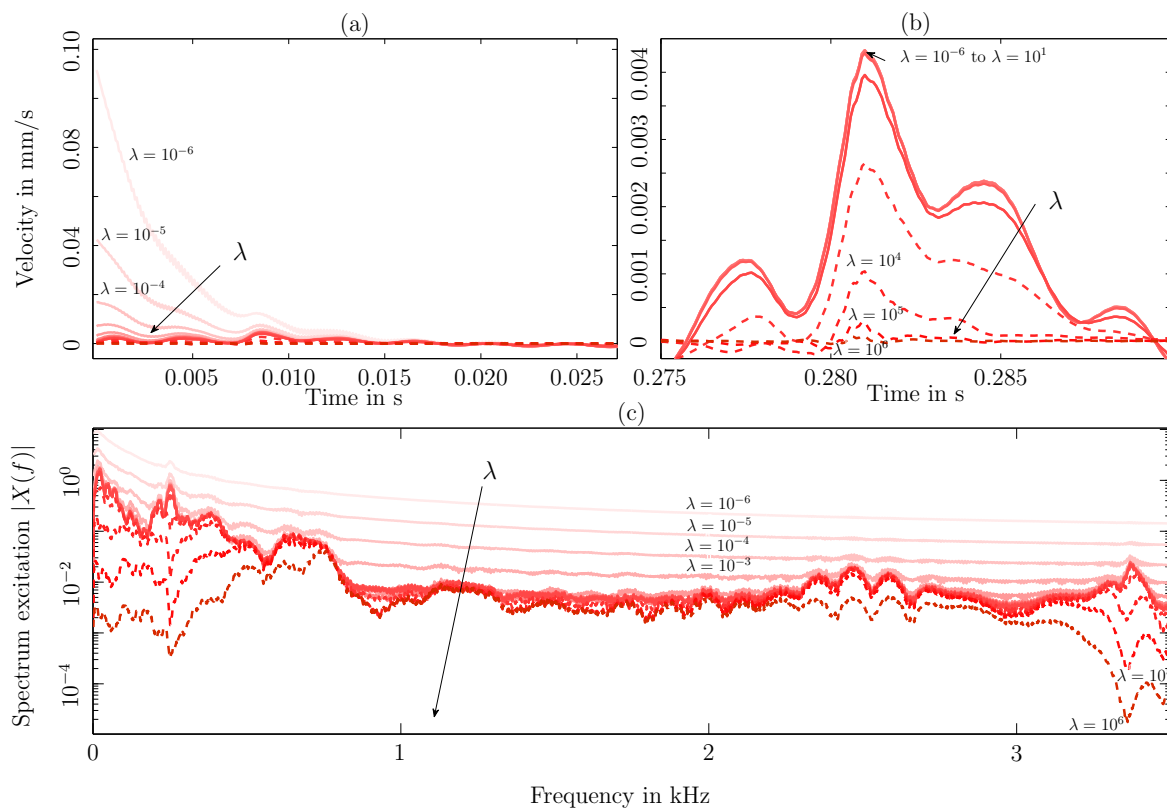


Figure 4 – Variation of parameter  $\lambda$  and effect on the (a) excitation signal (velocity) at the beginning of sampled time series segment of *Iridomyrmex purpureus* and (b) and somewhere in-between; (c) spectra of excitation from 0 to 6 kHz; arrows point in direction of increasing  $\lambda$ .

The ant signal was deconvolved using the transfer function of the veneer disc. However, deconvolution, even for computational data and even more so for real life measured data (inverse filtering), is an inverse problem which could lead to singular or ill-conditioned matrices causing serious signal distortion and artefacts. Attempts of signal enhancement with deconvolution can be found in image processing with a point-spread function using wavelet filtering in combination with soft/hard thresholding (regularisation) (30). Another well established method often used in geoscience is the water level method or also the TIKHONOV regularisation (or statistical ridge regression, WIENER filtering) which both work similarly by adding uncorrelated noise and by modifying the denominator in order to improve the condition of the matrix.

Here we use TIKHONOV regularisation. Let  $\mathbf{X}$  be the Discrete Fourier Transform of the desired excitation signal (complex vector),  $\mathbf{G}$  be the transfer function of the veneer disc and  $\mathbf{Z}$  be the measured and filtered response of the ants. Minimisation of the EUCLIDEAN norm of the difference  $\varepsilon^2 = \|\mathbf{X} \cdot \mathbf{G} - \mathbf{Z}\|_2^2$  gives an estimate of  $\mathbf{X}$ , which might be nearly always overdetermined, so a so-called TIKHONOV matrix (as

regularisation matrix) can be incorporated which leads to the following expression in the excitation signal.

$$\mathbf{X} = \{\bar{\mathbf{G}} \circ \mathbf{Z}\} \oslash \{(\bar{\mathbf{G}} \circ \mathbf{G} + \Gamma) \cdot dt \cdot \mathbf{1}\} \quad (3)$$

with  $\bar{\mathbf{G}}$  being the conjugated transfer function,  $dt$  the time step size,  $\circ$  and  $\oslash$  the HADAMARD product and its inverse operation (elementwise division) and  $\Gamma = \lambda \mathbf{1}$  being the regularisation matrix equal to an arbitrary regularisation parameter  $\lambda$  times a vector with only ones  $\vec{1} = \mathbf{1}$  (31) (for matrix operation this would be the identity matrix  $I$ ). The factor  $\lambda$  has been set to  $10^{-6}$  to avoid singularities when  $\mathbf{G}$  is very close to zero at a particular frequency;  $\lambda$  was chosen to be constant as the noise level of the laser vibrometer measurements was very low and not changing much between measurements.

A variation of  $\lambda$  from  $10^{-6}$  to  $10^6$  in  $10^1$  steps was conducted in a second TIKHONOV regularisation to retrieve the excitation signals. Figure 4 (a) shows that for the measurements considered (here of *Iridomyrmex purpureus*) for very small  $\lambda$  at the beginning of the inverse Discrete FOURIER Transform, low frequency distortion is induced but attenuates for  $\lambda > 10^{-2}$ . Figure 4 (b) shows that the effect on the excitation signal away from the end samples of the time series segment is not significant if  $\lambda \leq 10^2$ ; for greater values of  $\lambda$  the deconvoluted signal amplitude attenuates quickly. Figure 4 (c) indicates that only for a chosen  $\lambda$  between  $10^{-1}$  and  $10^2$  the spectrum does not change very much. Therefore  $\lambda = 10^1$  was chosen with maximum elimination of low frequency distortion and minimal changes of excitation amplitudes and spectral content. Please note that the decision on the choice of the value of the regularisation parameter  $\lambda$  has been based on comparing spectra within the frequency interval 0.1 to 3.5 kHz (see coherence in Figure 2). After deconvolution the time series was again nonlinearly filtered to estimate the time delay and the embedding dimension using the averaged auto-mutual information and the global false nearest neighbour algorithm. Details of this procedure given in the next section.

#### 4. EXCITATION SIGNAL OF ANT SPECIES

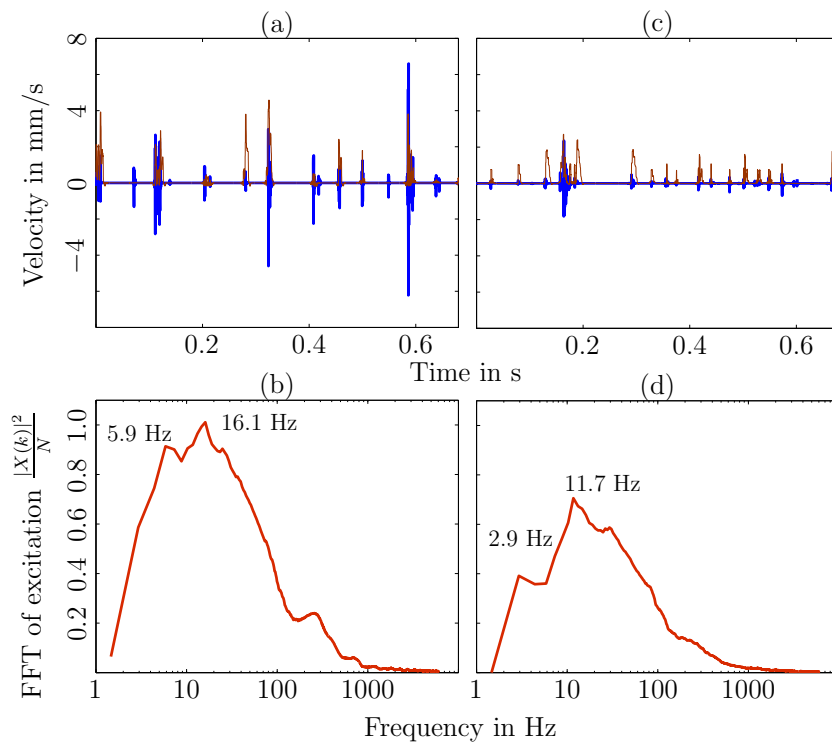


Figure 5 – Comparison of ant excitation and response signals (time traces & excitation spectrum) (a) & (b) *Iridomyrmex purpureus*; (c) & (d) *Lasius niger*

For *Iridomyrmex purpureus* a delay of  $\tau = 24$  samples was determined (bin width 10) with a minimum embedding dimension of  $m = 5$  (0 % false neighbours!) using the maximum norm and a possibly infinite neighbourhood. For *Lasius niger* the delay was  $\tau = 28$  samples with  $m = 4$ . The nonlinear noise reduction algorithm was subsequently applied with 4 iterations and 69.23 % of the standard deviation as the neighbourhood size. Results of the excitation signal and the response signal together with the excitation response are

given in Figure 5.

*I. purpureus* response signal compared to that of *L. niger* has almost double as large a velocity amplitude while its excitation signal has approximately the same level of magnitude to the excitation signal of *L. niger*; the fundamental frequency is 16.11 Hz with about a subharmonic frequency of 5.859 Hz. For the smaller ant species *L. niger* the excitation signals are much larger in amplitude than the response signal and on average about one third of the amplitude of that of *I. purpureus*. The frequency spectrum of *L. niger* shows a fundamental frequency of 11.72 Hz and a subharmonic component of 2.93 Hz.

Even though the coherence of the transfer mobility indicates that measurements below 35 Hz (coherence less than 0.6 and about 0.96 above 53 Hz) are not reliable due to the limitation of the loudspeaker as an excitation source, the choice of a proper TIKHONOV parameter value in combination with the nonlinear filtering based on the dynamics in phase space is able to extract the excitation signal.

Figure 6 (a) depicts the median signal of all excitation signals (lying in  $2^{13}$  samples) above the average noise level threshold amplitude, normalised, centred and finally multiplied by the median amplitude for *I. purpureus* and *L. niger*. The excitation of *I. purpureus* has approximately double the amplitude of that of *L. niger* which is in agreement with Figure 5. Both median excitations indicate plateaus similar to stepping functions. Figure 6 (b) shows one typical signal of *I. purpureus* which indeed looks like a step function smoothed out in the process of averaging a single step.

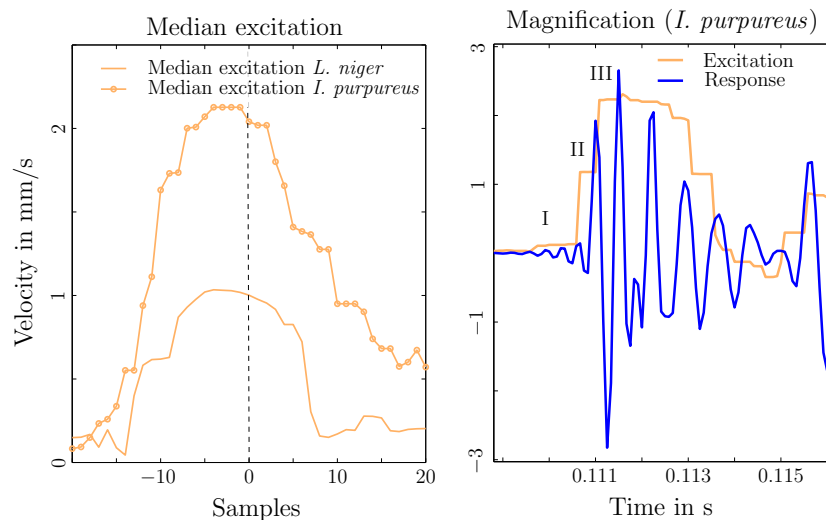


Figure 6 – Magnified area of excitation and response signal of one single individual of *I. purpureus* of the time trace depicted in Figure 5(a).

## 5. DISCUSSIONS

Recent detailed analysis of vibrations caused by ants activity on a thin substrate have been conducted (16), which was however not sensitive enough to detect a walking impact. Previous articles concerned with ant walking (22, 23, 24) only analysed qualitatively or visually the motion of ants. These issues were overcome in the present analysis by (1) measuring the transfer function of the veneer disc contact-less (hence without mass loading the structure) using laser vibrometry, with the environmental noise being minimised using a passive vibration control air cushioned bench top in an anechoic chamber (c.f. Oberst et al. (16)) and by (2) applying inverse signal processing to extract the excitation.

Compared to Nava-Baro et al. (17) using wavelet filtering, the application of nonlinear filtering techniques based on the description of the dynamics in phase space performs better. Wavelet filtering is limited in the types of signals to be approximated as only one mother wavelet can be chosen, even though the choice should be adaptive depending on the signal type and strength. Wavelets introduce oscillations which contaminate the filtered signal owing to decomposition and subsequent wavelet synthesis using a finite number of scales.

The deconvolution process uses *Tikhonov* to regularise the singularity due to the division of zero (extraction of transfer function) and remedies the ill-conditioned matrices for extracting the excitation signal. The regularisation parameter  $\lambda$  should be carefully monitored; an adaptive choice of  $\lambda$  was not necessary as the noise level was well controlled.

The excitation signal due to ants walking shows an amplitude growing step function. Ants are known to walk in a wavelike motion in a tripod pattern e.g. L1R2L3 (first leg left, second leg right) then R1L2R3

and so forth (23). The excitation signal in Figure 6 shows that the time the first foot seems to stay on the veneer is 0.8 ms for e.g. L1, 0.4 ms for L1 + R2 and then 1.5 ms for L1+R2+L3 with the whole process of setting the foot down and lifting it up taking 3.4 ms. The fundamental frequency of the walking signal for *Iridomyrmex purpureus* is 16 Hz and 12 Hz for the smaller ant *Lasius niger* which is of the same order of magnitude reported in (22).

## 6. CONCLUSIONS

Our results show for the first time that the excitation signal owing to ants' walking on a thin veneer disc can be extracted from the disc vibrations using deconvolution techniques in combination with nonlinear filtering based on the dynamics in phase space. Micro vibrations on a thin veneer disc arising from ants walking were recorded with a vibration isolated laser vibrometer in an anechoic room. In order to further reduce the noise contained in the measurements, the recorded vibrations were filtered with non-linear statistical filtering based on the dynamics in phase space before the excitation signal was deconvolved from the veneer response by applying TIKHONOV regularisation (via adding controlled noise to the spectrum). The extracted footstep pattern shows the tripod motion of ants in form of a step function. The fundamental frequency of the ants is 12 and 16 Hz. However, more research is necessary to validate the footstep pattern for different ant species and to optimise the deconvolution process in order to understand walking of ants better by statistically analysing the excitation signal to obtain an average foot step pattern.

## ACKNOWLEDGEMENTS

This research was supported under Australian Research Council's Discovery Projects funding scheme (project number DP110102564). We acknowledge the special research permit for research-conditions granted by the Forestry Corporation of NSW (FCNSW). The first author received an ECR travel grant provided by the AAS NSW Division.

## REFERENCES

1. Wiener N. *Cybernetics: or Control and Communication in the Animal and the Machine*. The Massachusetts Institute of Technology; 1965.
2. Hölldobler B. Multimodal signals in ant communication. *Journal of Comparative Physiology A: Neuroethology, Sensory, Neural, and Behavioral Physiology*. 1999;184:129–141.
3. Trong Nguyen T, Akino T. Worker aggression of ant *Lasius japonicus* enhanced by termite soldier-specific secretion as an alarm pheromone of *Reticulitermes speratus*. *Entomological Science*. 2012;15(4):422 – 429. Available from: <http://dx.doi.org/10.1111/j.1479-8298.2012.00534.x>.
4. Jackson DE, Ratnieks FLW. Communication in ants. *Current Biology*. 2010;16:1–5.
5. Kretz R. Ants can outsee us all. *New Scientist*. 1979;83:656f.
6. Narendra A, Reid SF, Hemmi JM. The twilight zone: ambient light levels trigger activity in primitive ants. *Proceedings of the Royal Society B: Biological Sciences*. 2010;277(1687):1531–1538.
7. Narendra A, Reid SF, Greiner B, Peters RA, Hemmi JM, Ribi WA, et al. Caste-specific visual adaptations to distinct daily activity schedules in Australian *Myrmecia* ants. *Proceedings of the Royal Society B: Biological Sciences*. 2011;278(1709):1141–1149.
8. Evans TA, Lai JCS, Toledano E, McDowall L, Rakotonarivo S, Lenz M. Termites assess wood size by using vibration signals. *Proceedings of the National Academy of Sciences of the United States of America*. 2005;102(10):3732–3737.
9. Evans TA, Inta R, Lai JCS, Prueger S, Foo NW, Fu EW, et al. Termites eavesdrop to avoid competitors. *Proceedings of the Royal Society B: Biological Sciences*. 2009;276(1675):4035–4041.
10. Roces F, Tautz J. Ants are deaf. *The Journal of the Acoustical Society of America*. 2001;109(6):3080–3082. Available from: <http://link.aip.org/link/?JAS/109/3080/1>.
11. Buehlmann C, Hansson BS, Knaden M. Desert Ants Learn Vibration and Magnetic Landmarks. *PLoS ONE*. 2012 03;7(3):e33117.

12. Masters WM, Tautz J, Fletcher NH, Markl H. Body vibration and sound production in an insect (*Atta sexdens*) without specialized radiating structures. *Journal of Comparative Physiology A: Neuroethology, Sensory, Neural, and Behavioral Physiology*. 1983;150:239–249. 10.1007/BF00606374. Available from: <http://dx.doi.org/10.1007/BF00606374>.
13. Roces F, Hölldobler B. Vibrational Communication between Hitchhikers and Foragers in Leaf-Cutting Ants (*Atta cephalotes*). *Behavioral Ecology and Sociobiology*. 1995;37(5):297–302. Available from: <http://www.jstor.org/stable/4601143>.
14. Meyhöfer R, Casas J. Vibratory stimuli in host location by parasitic wasps. *Journal of Insect Physiology*. 1999;45(11):967 – 971.
15. Sala M, Casacci LP, Balletto E, Bonelli S, Barbero F. Variation in Butterfly Larval Acoustics as a Strategy to Infiltrate and Exploit Host Ant Colony Resources. *PLoS ONE*. 2014 04;9(4):e94341.
16. Oberst S, Lai JCS, Evans TA. Vibration as a means of quantifying ant activity in laboratory experiments. *PLoS ONE*. 2014;9(3):e90902.
17. Baro EN, Oberst S, Lai JCS, Evans TA. A signal processing method for extracting vibration signals due to ants' activities. In: *Internoise 2013, Innsbruck, Austria, 15.-18. September, 2013*. p. 1–10.
18. Easterling KE, Harrysson R, Gibson LJ, Ashby MF. On the Mechanics of Balsa and Other Woods. *Proceedings of the Royal Society of London A Mathematical and Physical Sciences*. 1982;383(1784):31–41.
19. Full RJ, Tu MS. Mechanics of six-legged runners. *Journal of experimental biology*. 1990;148:129 – 146.
20. Fischer H, Schmidt J, Haas R, Büschges A. Pattern Generation for Walking and Searching Movements of a Stick Insect Leg. I. Coordination of Motor Activity. *Journal of Neurophysiology*. 2001;85(1):341–353. Available from: <http://jn.physiology.org/content/85/1/341>.
21. Goldschmidt D, Wörgötter F, Manoonpong P. Biologically-inspired adaptive obstacle negotiation behavior of hexapod robots. *Frontiers in Neurorobotics*. 2014;8:3.
22. Zollikofer CPE. Stepping pattern in Ants, I. Influence on speed and curvature. *Journal of experimental biology*. 1994;192:95 – 106.
23. Zollikofer CPE. Stepping pattern in Ants, II. Influence of body morphology. *Journal of experimental biology*. 1994;192:107–118.
24. Zollikofer CPE. Stepping pattern in Ants, II. Influence of load. *Journal of experimental biology*. 1994;192:119 – 127.
25. Oberst S, Lai JCS, Evans TA. Novel method for pairing wood samples for choice tests. *PLoS ONE*. 2014;9(2):e88835.
26. Mailleux AC, Buffin A, Detrain C, Deneubourg JL. Recruitment in starved nests: the role of direct and indirect interactions between scouts and nestmates in the ant *Lasius niger*. *Insectes Sociaux*. 2011;58:559 – 567.
27. Abarbanel HDI. *Analysis of observed chaotic data*. Springer: New York; 1996.
28. Schreiber T. Extremely simple nonlinear noise reduction method. *Physical Review E*. 1993;47:2401–2404.
29. Hegger R, Kantz H, Schreiber T. Practical implementation of nonlinear time series methods: The TISEAN package. *Chaos: An Interdisciplinary Journal of Nonlinear Science*. 1999;9(2):413–435. Available from: <http://link.aip.org/link/?CHA/9/413/1>.
30. Grace Chang S, Yu B, Vetterli M. Adaptive Wavelet Thresholding for Image Denoising and Compression. *IEEE TRANSACTIONS ON IMAGE PROCESSING*. 2000;9:1532– 1546.
31. Tikhonov A, Arsenin VY, John F. *Solutions of ill-posed problems*. John Wiley & Sons, New York, Toronto, London, Sydney; 1977.